ELSEVIER

Powder Technology 112 (2000) 111–125

POWDER TECHNOLOGY

www.elsevier.com/locate/powtec

Magnetically mediated flow enhancement for controlled powder discharge of cohesive powders

Rajesh N. Dave [a,*], Chang-Yu Wu [b], Bodhisattwa Chaudhuri [a], Satoru Watano [c]

[a] *Particle Processing Research Center, Department of Mechanical Engineering, New Jersey Institute of Technology, Newark, NJ 07102-1982, USA*
[b] *Department of Environmental Engineering, University of Florida, Gainesville, FL 32611, USA*
[c] *Department of Chemical Engineering, Osaka Prefecture University, 1-1 Gakuen-cho, Sakai, Osaka 599-8531, Japan*

Abstract

A new flow enhancement system is developed for cohesive powders. It is based on the concept of multiple, point source, internal excitations. In this system, a mass of small permanent-magnetic particles are placed in the discharge zone of a hopper, and then an oscillating magnetic field is applied to excite these magnets. A screen is placed at the exit to keep the magnets within the hopper. The magnetic particles spin furiously, go though random collisions with each other, and agitate the mass of cohesive powder near the exit of the hopper. As a result, the internal structure of the cohesive powder is disrupted and the powder gets fluidized and demonstrates an increased flowability. This device, called the magnetically assisted powder flow (MAPF) system, has been investigated for discharging cohesive powder from a hopper. It is shown that this device is capable of a controlled powder discharge, which is a linear function of time. The effects of various parameters, such as the amount and size of the magnetic particles and the magnetic field strength on the discharge rate are investigated. The operating principle of this device is different from conventional flow enhancement devices such as pneumatic, vibrational, or mechanical systems because powder ''fluidization'' is generated through random motion of the magnetic particles within the powder, and the presence of the screen prevents flooding. Modeling of the motion of the magnetic particles under the influence of an oscillating field is considered to show how the spinning and random translations occur in such a system. Discrete element modeling of a system of magnetic particles is also carried out to show the effect of various parameters on fluidization. This system can be applied for other powder technology applications, for example, the measurement of angle of repose for cohesive powders.

Keywords: Hopper flow enhancements; Magnetic fluidization; Angle of repose; Discrete element simulations

1. Introduction

In most industrial applications requiring the handling and/or processing of granular materials or powders, these materials are often stored in devices such as bins or silos, both before and after processing. When the material must be taken out from the containers, the delivery is made through discharge from hoppers. The problems with the discharge (based on gravity flow or other means) are well known [1–13], and have frequently been the subject of many research papers [14–23]. While some progress has been made for gravity flow out of hoppers based on the theory of geometric hopper design [1,2], much remains to be done for high value-added specialty applications (pharmaceuticals, cosmetics, ceramics) that deal with small batch processes involving a wide variety of raw materials. This is because the design based on a Jenike-type procedure [1] may not be applicable to many of these applications, since the small batch size often makes the minimum outlet dimension requirement imposed by the Jenike procedure unrealizable. Moreover, these industries require devices that produce predictable and controllable amount of flows and avoid segregation upon delivery. When the bulk material is cohesive, the gravity flow out of a hopper is difficult or even impossible even with some modifications to the hopper's geometry [8]. This requires the use of active discharge aids [8,13]. While some of these methods may be effective for certain situations, for many cases they may not work properly and even cause additional problems. These problems include uncontrollable flow, flooding, dust explosion, damage to hopper walls, segregation

* Corresponding author. Tel.: +1-973-596-3352; fax: +1-973-642-4282.
E-mail address: dave@njit.edu (R.N. Dave).

0032-5910/00/$ - see front matter
PII: S0032-5910(99)00312-5

upon discharge, increased powder compaction, etc. [4,6,8,9,13,15].

The most serious problem in hopper discharge is the no flow condition, and it occurs due to either rat-holing or arching. Rat-holing generally occurs due to high friction between the hopper walls and the material and/or due to cohesion of the material under consolidation. Arching can occur due to mechanical interlocking, or more frequently due to the cohesive strength of the solid. Normally, this can be overcome by increasing the outlet size. The conventional wisdom dictates that, if at all possible, one should design a mass flow (or in some cases, expanded flow [12]) hopper, based on the Jenike procedure, which determines both the slope and the outlet of the hopper to prevent arching and rat-holing problems. However, if the conditions imposed by this design cannot be met, then other options are required. As mentioned before, a variety of flow enhancements or hopper modifications have been proposed. In the following paragraphs, the main features and principles of these are described.

1.1. Existing flow enhancement techniques

To combat flow problems in existing hoppers, certain modifications can be made. These range from simply altering the flow properties of the powder using chemical additives to installing air blasters that break stable arching. Chemical additives are usually coated on each particle and promote flow by reduced inter-particle adhesion. These may be dry powders such as silicates, stearates, or phosphates. In some applications, the use of such additives may not be compatible. Wall friction may be reduced by using liners such as ultra-high-molecular-weight polyethylene or polished stainless steel sheets. In certain cases, inserts such as ''hopper-within-a-hopper'' are used [23] to achieve mass flow hoppers. These can help when the existing hopper does not have the required slope for mass flow. However, if the hopper outlet is smaller than what is required for mass flow, then this option is not useful. If passive means cannot help in improving the flow situation, active or energy-input type discharge aids may be required. There are three categories of these devices: pneumatic, vibrational, and mechanical. These are described below.

In pneumatic methods, one can use aeration, air-blasts, or air-inflators. In aeration, a controlled amount of air is introduced in the bulk, at either a high-level or low-level aeration. In high-level aeration, the amount of air is sufficient to reduce wall friction and to make the material near the outlet aerated to flow like a liquid. While this may work for some conditions, it may cause flooding for others. In low-level aeration, the amount of air introduced is low, but enough to encounter de-aeration due to time consolidation. This prevents the flooding problem, but it cannot improve the situation where even the freshly introduced material has difficulty flowing out of the hopper. In air-blasting methods, a small quantity of high-pressure air is injected into the bulk in sudden bursts. This may impart shocks which could break an arch or a rathole. While there are documented cases [7] of the utility of this approach, others caution against such a technique [8] and recommend its use as a last resort. Other pneumatic devices utilize inflatable pads mounted along the hopper walls, which are activated at regular time intervals. These devices may break arches and cause flow to occur. However, it is believed that for highly cohesive materials, these techniques can cause further problems due to increased compaction.

In vibrational techniques, there are two different approaches. In the first approach, the vibrations are applied to the hopper wall. One or more vibrators are mounted directly on the hopper wall. The utility of these have been questioned [5,8,13] mainly because these devices may fail to transmit the vibration where needed, and in some cases, further compact the material [15]. It is recommended that these should be never operated while the outlet is closed. In the second approach, mounted vibrating devices agitate the entire powder bulk near the outlet. These fall loosely in the category of bin activators [3,5,8,13], of which various kinds are commercially available. It is argued that these devices provide a ''live'' bottom at the outlet, and can easily handle most flow problems [8]. It is usually recommended that these devices be operated on a cycle of on and off times.

In mechanical methods, an arm or a screw moves inside the bulk and it continuously acts against a stable formation of an arch or a rat-hole. These devices may work very well for certain types of materials and hoppers. However, for very large silos containing highly cohesive materials, the solids pressure may be excessive, resulting in high stresses upon the devices and requiring large power to operate [5].

While there are many techniques for improving hopper flows as described above, they are essentially based on enhancement of the flowability of the material, or reduction in the wall friction, or both. The wall friction is reduced by passive (e.g., liners) or active (e.g., wall vibration) means. The material flowability is improved by chemical additives, aeration, or agitations. The main idea is to decrease inter-particle adhesion by passive means or by energy input. While it may be possible to characterize or quantify the effect of wall friction reduction by passive means or the effect of improved flowability due to chemical additives on the hopper flow, it is not easy to do so for active means of flow enhancements. Some guidelines to do so for vibration effects have been proposed by Roberts et al. [14], but it is assumed that the entire powder bulk in the hopper is vibrating under the same conditions as that of the test. There have also been several other studies of hopper material undergoing vibrations [15–21]. However, these studies utilize non-cohesive particles, and in general are concerned with the vibration of the whole hopper. Thus, these investigations do not have a direct relation to popular devices. Moreover, while it is well known that vibration can facilitate granular flows, it can also cause size segrega-

tion [20], and the use of certain levels of vibrations in a storage container or hopper can lead to material compaction and hence reduced flowability [15].

Nevertheless, from the preceding it is clear that in general the flow aid must either reduce the wall friction, or improve the flowability of the powder (or do both). The ways in which this is accomplished is different for different techniques. The main difficulty in most of the techniques described here relates to their ability in transmitting the applied energy to a large portion of the bulk in a uniform and controlled manner. For example, it is not clear if the vibrations applied to the wall are transmitted within the bulk to effectively reduce inter-particle cohesion. Similarly, in aeration, it is not clear if the air diffuses evenly within the bulk or forms large bubbles and finds easy channels to get to the top of the hopper instead. For instance, in the field of fluidized beds, it is well known that a certain class of powders cannot be easily fluidized and some are subjected to bubbling.

In this paper, we present a novel method that is based on magnetic fluidization. In this technique, the agitations are applied through violent spinning of a mass of magnetic particles placed within the powder bulk. In contrast to most techniques that are based on either single or a limited number of sources of energy input, this device is capable of providing excitation at a very large number of locations near the outlet of the hopper. In this system, magnetic particles act as the internal media to break the arch or the rat-hole. Moreover, it will be shown that by using this approach, a controlled powder flow rate can be achieved by adjusting parameters such as the magnetic mass, magnet size, and magnetic field strength. In the next section, this system is described in detail.

2. Magnetically assisted powder flow (MAPF) system

A schematic of the MAPF system is shown in Fig. 1. As shown, the magnets and the powder to be fluidized are placed in a hopper, with its outlet covered by a mesh to keep the magnetic particles from flowing out. These magnetic particles are agitated by a time varying external electromagnetic field, which can be controlled by adjusting the input voltage to the field coil. The furious agitation of the magnetic particles causes them to break the powder structure, inducing the powder flow. It was observed under high-speed digital video that the principal magnet motion is its rotation, and the secondary effect is a random motion due to collisions with the wall and other particles. This in turn creates shear and fluidization within the powder. While magnetic means have been used in fluidized beds before [24,25], the principle of fluidization in this system is different. In the magnetic fluidized bed system [24,25], the media particles are made of ferromagnetic material having high permeability and low coercivity, and thus, are soft magnets. Thus, under the influence of a magnetic field, the particles get magnetized. The magnetic field is not time varying, and thus the soft magnetic particles create chains (acting like rubber-bands) within the bed in order to break down the bubbles. That in turn creates a magnetically stabilized fluidized bed. In contrast, our system utilizes hard permanent magnets with low permeability and high coercivity. The applied magnetic field is time varying. Hence, the particles spin and move under the effect of the magnetic field within the powder to make it fluidized. Thus, the concept of fluidization in our system is drastically different from the one in Refs. [24,25]. Each magnetic particle draws energy from the field and acts as a source of internal excitation, causing fluidization. Such fluidization ability has been used for other applications such as mixing, grinding [26–28], and dry particle coating [29,30]. However, we present, for the first time, its use in powder flow enhancement.

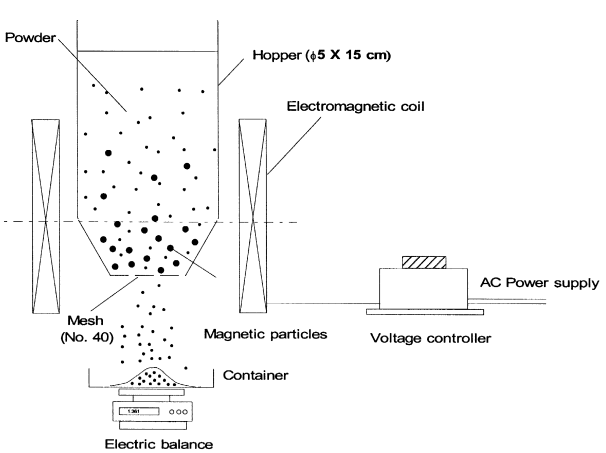

Fig. 1. Schematic of the MAPF system for powder discharge.

To show the effect of magnets on fluidization, a simple experiment is considered. A mass of 0.5 g of magnets is mixed with about 2 g of cornstarch in a small bottle with 1.2 cm diameter. In its unfluidized state, this is shown in Fig. 2. As can be seen, the mixture of the magnets and cornstarch occupies a small fraction of the volume of the bottle. When the magnetic field is turned on, the magnets spin and move randomly, and fluidize the mixture. Fig. 3 shows the picture of fluidization. As can be seen, the fluidized mixture fills up the whole bottle. In a hopper, the effect is somewhat different. Instead of a rise in the level of the powder, the material is simply forced out through the bottom outlet of the hopper. This fluidization can be explained through examining the governing equations of motion. In the next section, we present these equations for a system of magnetic particles.

2.1. Governing equations

Each magnetic particle is treated as a small magnetic dipole for the sake of simplicity. The magnetic dipole

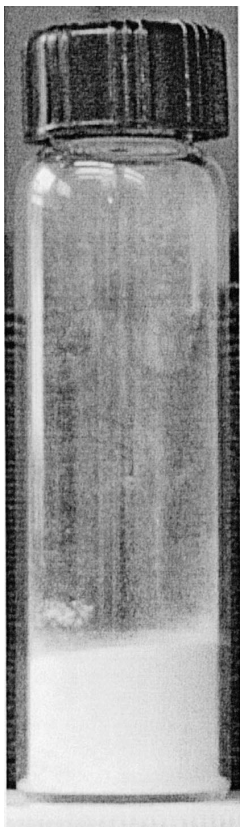

Fig. 2. Mixture of magnets and cornstarch before application of the magnetic field.

moment for a typical barium ferrite particle used in our experiments when properly magnetized under a field strength of approximately 0.15 T is 0.52 emu. When these particles are subjected to an external oscillating magnetic field, the amount of actual magnetization will change and there will be a hysteresis effect. However, for the sake of simplicity it is assumed that these particles have a constant magnetic dipole moment. Then the torque, $\boldsymbol{T}_{\text{ext}}$, existing on a magnetic particle due to the external field is given by

$$\boldsymbol{T}_{\text{ext}} = \boldsymbol{m} \times \boldsymbol{B}_{\text{external}} \tag{1}$$

where $\boldsymbol{m}$ is the magnetic dipole moment of the particle, and $\boldsymbol{B}_{\text{external}}$ is the magnetic flux density of the external field. While the exact expressions for the magnetic flux density in a finite sized field coil are complex, our first assumption is to consider the coil as an infinite length solenoid. Thus, the $\boldsymbol{B}_{\text{external}}$ is given by

$$\boldsymbol{B}_{\text{external}} = \mu_0 NI\hat{\mathbf{k}} \tag{2}$$

where μ_o is the permeability, N is the number of turns per meter in the coil, I is the current in the coil, given by $I = I_0 \sin(\omega t)$, and $\hat{\boldsymbol{k}}$ is the unit vector in the direction of the solenoid axis. Since the current oscillates at the frequency of ω, the external field also oscillates at the same frequency. Thus, the torque (Eq. (1)) acting on the particle is time varying. If the torque was constant, a magnetic particle would tend to align itself with the flux and in the presence of any damping effects, it would eventually come to rest. However, since the flux is time-variant, its direction continuously switches, and the magnetic particle may not come to rest under small damping. As a result, the applied torque would cause the particle to spin. Apart from the effect of external field, particles themselves generate a magnetic field around them, and that field varies strongly with spatial position. This dipole–dipole induced flux density, $\boldsymbol{B}_{\text{dipole}}$ is given by

$$\boldsymbol{B}_{\text{dipole}} = \frac{\mu_0}{4r^5\pi}\left[3(\boldsymbol{m} \times \boldsymbol{r})\boldsymbol{r} - r^2\boldsymbol{m}\right] \tag{3}$$

where the vector $\boldsymbol{r}$ is the position where the field is computed with respect to the dipole coordinate system and $\boldsymbol{m}$ is the magnetic dipole moment. Due to this field, in addition to generating a net torque, there is also a net magnetic force on the particle and the particle is subjected to translation in addition to rotation. The net force, $\boldsymbol{F}$, acting on a magnetic particle due to the combined magnetic flux, $\boldsymbol{B}$ is

$$\boldsymbol{F} = \nabla(\boldsymbol{m} \times \boldsymbol{B}) \tag{4}$$

and the net torque, $\boldsymbol{T}$ on a particle is

$$\boldsymbol{T} = \boldsymbol{m} \times \boldsymbol{B} \tag{5}$$

where $\boldsymbol{B}$ is the total magnetic flux density, which includes the external field. In case of a solenoid and a single

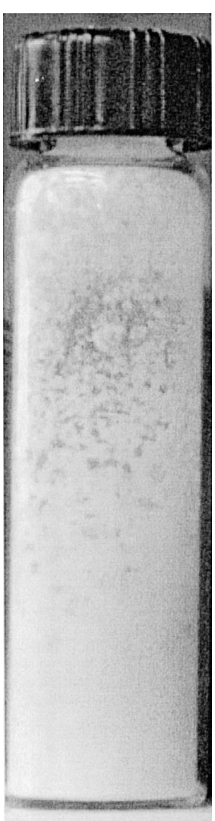

Fig. 3. Mixture of magnets and cornstarch after application of the magnetic field.

magnetic particle, the magnetic flux density is uniformed in space, hence there is no net magnetic force on the particle and there is only a net torque given by Eq. (1). Thus, a simple equation for the rotational motion of a particle is

$$J\ddot{\boldsymbol{\theta}} = \boldsymbol{m} \times \boldsymbol{B}. \quad (6)$$

While not clear in the above form, Eq. (6) is highly non-linear. We note that in a real situation, the magnetic flux density due to an external coil is not uniform, hence, the particle is subjected to additional magnetic force. From the equations above, it is evident that as a result of the combined effect of all magnetic interactions, the particles spin, translate, and collide with the walls of the container and with other particles. These collisions eventually fluidize the whole system of magnetic particles. When other particles (non-magnetic, e.g., powder to be fluidized) are present along with the magnetic particles, the spinning and translation results in fluidization along with the development of local micro-shear zones. This could cause reduction in the bulk strength of the material and flow would occur.

The above governing equations are incorporated into a discrete element computer simulation code and initial results for fluidization of the magnetic particles are obtained. The simulation is based on code developed originally in Refs. [31–33], which utilizes the ideas proposed in Ref. [34] based on the extension of molecular dynamics modeling. In these simulations, the powder particles are assumed to be spherical and exhibit elastic–plastic behavior with frictional contacts. Thus, the contacts are modeled as soft sphere interactions including friction. Various details of these simulations are presented elsewhere. Our contribution involves incorporation of magnetic particles and corresponding forces and torques. The results of the simulation study will follow the results of the experimental study.

3. Experimental study

For all the experiments, the magnetic particles (barium ferrite — $BaO–6Fe_2O_3$ — coated with Polyurethane, Aveka; 0.85–3 mm) together with the powder (cornstarch, Argo; mean diameter = 15 μm) were placed inside the cylindrical hopper (Plexiglas). Two hopper geometries were used: a cylindrical flat-bottom bin and a conical hopper with a 60° inclination. The inclination angle was measured with respect to horizontal axis. The hopper diameter and height were 5 and 15 cm, respectively. In the cylindrical bin configuration, the hopper outlet was also 5 cm, while in 60° inclination configuration, the outlet diameter was 2.5 cm. The reason for considering a flat-bottom cylindrical hopper was due to the fact that the effect of the hopper angle is eliminated, and this represents the best condition for flow (barring the limitation of the size of the outlet). Even under that condition, there was no flow out of the hopper for a cohesive material such as cornstarch without any external energy input. The bottom of the hopper was positioned 1 cm below the centerline of the magnetic field as shown in the figure. The outlet of the hopper was covered by a fine mesh (No. 40, North Wire Clothes-635 μm opening) to keep the magnetic particles in the system while the fine powder could be discharged through the mesh.

Various system parameters affect the discharge from the hopper. These were varied to investigate the effectiveness of the MAPF system on the discharge of cohesive powder and to better understand its behavior. In this preliminary study, cornstarch was chosen as the representative cohesive material, which has a high angle of repose of about 60°. When this material was tested in a Jenike shear tester [1,2], the computations indicated a minimum outlet size of 1.2 m for a conical hopper. This further indicates that this is a very cohesive material for which arching could occur if the outlet is smaller than 1.2 m.

For each experiment, a fresh batch of cornstarch was taken. First, a series of experiments were conducted to study the mass flow out of the hopper as a function of time. Second, the effect of the amount of magnetic media on the mass flow rate was studied. This was followed by the evaluation of the effect of the external magnetic field strength and the size of the magnetic particles on the mass flow rate. Each set of experiments was repeated several times on the same day, and at least three measurements were made for each condition. The experimental conditions are listed in Table 1.

3.1. Mass flow as a function of time

In many applications, it is highly desirable that the flow rate out of the hopper is controlled. The MAPF system is capable of initiating the flow of cohesive powder material. In this series of experiments, its ability to discharge in a controlled manner was tested. A measured mass of the magnetic particles was initially placed at the bottom of the hopper and a measured quantity of cornstarch powder was filled above the magnetic particles. A variety of operating conditions, such as the magnetic field strength (varied by changing the input voltage), the amount of magnets, the size of the magnetic particles, and the location of the hopper within the magnetic field were considered. In all cases, a similar trend for mass flow as a function of time was observed. In Fig. 4, typical results are shown. Here, the discharged powder mass as a function of time is shown for 40 g cornstarch, 1 g magnetic particles, input voltage at 20 V, and straight bin hopper configuration with hopper outlet 1 cm below the mid-plane of the magnetic field. As seen in the figure, the variation of the mass flow is linear with time, except at the end of the discharge indicating a constant rate of discharge for this experiment. The error

Table 1
Experimental conditions for discharging unconsolidated powder using the MAPF system
Bulk density of unconsolidated corn starch: 0.79 g/cm^3. Hopper outlet from the magnetic field centerline: −1 cm. Initial placement of magnets: bottom. Total mass of cornstarch: 40 g (the flow rate is determined based on the time to deplete 36 g of cornstarch). Both flat bottom cylindrical bin and 60° hopper are used.

Parameter	Value		
	Set 1 (Fig. 5)	Set 2 (Fig. 6)	Set 3 (Fig. 7)
Magnet mass (g)	0.25, 0.5, 0.75, 1, 1.5, 2, 2.5, 3	1	1
Magnetic field strength controlled by power supply (V)	20	11, 12, 13, 14, 15, 16, 17, 18, 20, 22	20
Magnetic particle size (mm)	as received	as received	< 0.85, 0.85–1.18, 1.18–1.4, 1.4–1.7, 1.7–2, 2–2.36, > 2.36

bars indicate the variation of each observation, indicating very good repeatability. As mentioned before, similar results were obtained at different conditions, as well as in both of the hopper geometries, indicating that the geometry does not affect the result. These results show that this device is capable of not only initiating the flow of cohesive powder out of a very small (as compared to the ideal Jenike dimension) opening, but also achieving a constant discharge rate. Thus, it can also be used as an accurate powder feeder. Next, the results of varying several operating conditions are shown.

3.2. Powder flow rate as function of magnet mass

As shown in the previous set of experiments, the powder flow rate is constant for a given condition. However, a flow enhancement system should be also capable of changing the mass flow rate in a controlled manner. Amongst the various ways of changing the mass flow rate, a change in the amount of magnets is considered in this section. The ability of the magnets to fluidize the cohesive powder is due to the individual spinning motion as well as the multiple collisions and the ensuing random motion that takes place within the bulk. It is expected that as the amount of magnets in a fixed space is increased, the fluidization will be greater, and so will be the mass flow rate. This is examined for various conditions. In Fig. 5, results for both of the hopper configurations are shown. The other conditions for these results were an input voltage of 20 V, total cornstarch of 40 g with the mass flow rate measured for depletion of 36 g, and the hopper outlet 1 cm below the mid-plane. This figure shows a nearly linear increase in the mass flow rate in the range shown. As can be expected, the mass flow rate from the larger outlet of the straight bin configuration is higher (nearly twice) than that of the conical hopper. Each point on the curve is an average of at least three observations, and in several cases, error bars are smaller than the size of the plotted marker, indicating an excellent repeatability. While not shown in this figure, if the amount of magnets is increased significantly beyond 3 g, the flow rate started to decrease. This effect was more evident for the 60° conical hopper. This can be attributed to excessive activity of the

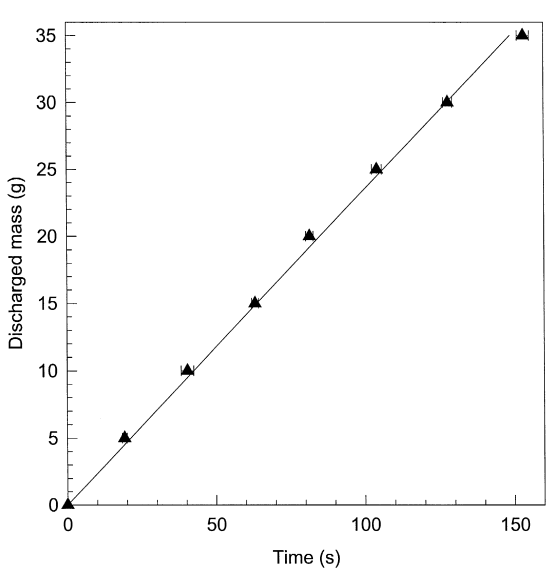

Fig. 4. Discharged powder mass as a function of time.

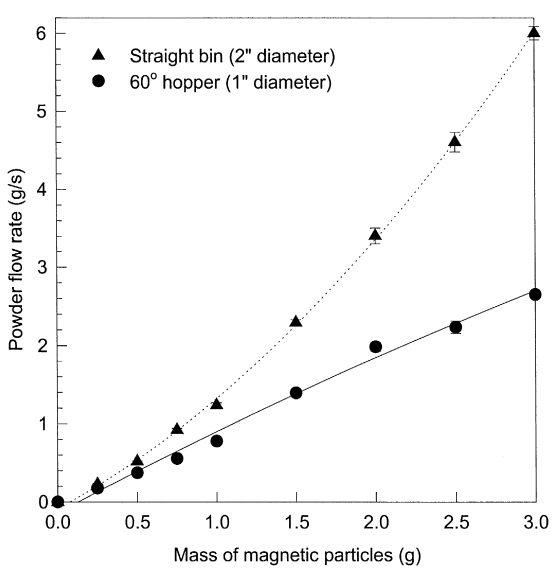

Fig. 5. Powder flow rate as a function of the total mass of magnetic particles.

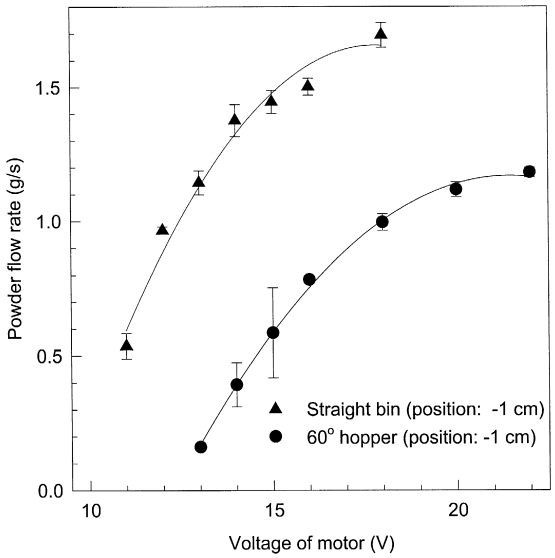

Fig. 6. Powder flow rate as a function of magnetic field strength (represented by applied voltage).

magnets, causing a very high level of collisions and fluidization such as to slow down the flow rate due to the prolonged suspension of the powder. This effect was more severe for the conical hopper, as the outlet was more restricted and the action of fluidization was more pronounced, inhibiting the discharge. However, in the useful range plotted in the graph, the behavior of the system is nearly linear and highly repeatable. This indicates that by adding more magnets (to a certain degree), the mass flow rate can be controlled. In the next section, variation in the magnetic field strength is considered as a means to control the flow rate.

3.3. Powder flow rate as function of magnet mass

The total amount of magnetic particles can be varied and thus different flow rates can be achieved as shown in the previous section. However, this way of controlling the mass flow rate is not very convenient on a real time basis. In this section, results of mass flow rate with change in the magnetic field strength as an operating parameter are considered. The results are shown in Fig. 6 for both of the hopper configurations. The other conditions for these results were mass of magnets 1 g, total cornstarch of 40 g with the mass flow rate measured for depletion of 36 g, and the hopper outlet 1 cm below the mid-plane. As seen in Eq. (2), the magnetic field strength is a direct function of the current flowing in the coil. In the system utilized here, the current could not be directly controlled. However, changing the coil voltage (which is related to the actual current flowing in the coil) could indirectly vary the magnetic field strength. Thus, the coil voltage was varied in this series of experiments. The results show a gradual rise in the discharge flow rate, until an optimum was reached. Although not shown in this figure, beyond that point, the flow rate began to drop. There could be several reasons for this. First, as the voltage is increased, the current may not always increase linearly, and thus, the magnetic field may not increase linearly as the voltage. This behavior was observed in the coil used in our experiments, and the magnetic flux density did not increase linearly with the voltage. The second reason is that while the magnetic flux density may not rise linearly, after a certain level, its effect could be causing excessive fluidization, thus causing the powder to be retained for a longer time in the hopper and thus slowing the mass flow rate. Moreover, the actual motion of the magnets and their subsequent effect on the powder motion is quite complex, so that a perfect linear relationship is not expected. However, due to the high repeatability of most of the observations, it is possible to use voltage levels as a means to control the flow rate once the system is calibrated.

3.4. Magnetic particle size

The size of the magnetic particles used affects the powder structure failure because the torque of the particle increases due to the higher magnetic moment as the particle size increases. Thus, it can also be used as one of the operating parameters to achieve a controlled flow rate. This effect was investigated by varying the magnetic particle size but keeping the total mass of the magnets constant. The results are shown in Fig. 7 by varying the nominal magnet size from 0.85 to 2.36 mm for both of the hopper configurations. The other conditions for these results were mass of magnet 1 g, input voltage 20 V, total cornstarch of 40 g with the mass flow rate measured for depletion of 36 g, and the hopper outlet 1 cm below the mid-plane. As shown in the figure, there is an optimum particle size to achieve the maximum powder flow rate. As mentioned

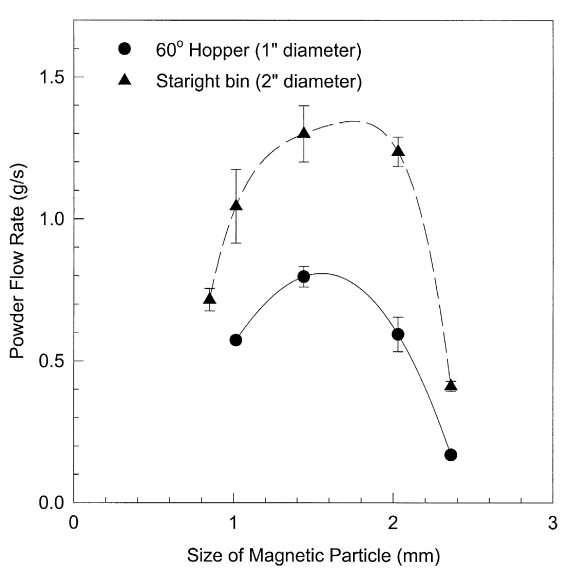

Fig. 7. Powder flow rate as a function of magnetic particle size for a constant total mass of magnets.

above, a larger magnetic particle has a higher magnetic moment. Hence, increasing the size can increase the powder flow rate by more effectively breaking the powder structure. On the other hand, the number of magnetic particles, hence the concentration of magnets within the same volume, is smaller for a larger particle size with the same total mass. Therefore, the frequency of collisions and hence powder structure failure is reduced when a very large particle size is used. Thus, the maximum flow rate is dependent on the optimum combination of the magnetic moment and the particle number concentration. For the conditions shown in the figure, the optimum magnet size is between 1 and 2 mm. The results of this study indicate that the size of the magnets may not be used as easily for control of the discharge rate as the amount of magnets. However, there is a need to select an optimum particle size for a given situation.

3.5. Angle of repose measurements using MAPF

While performing the powder discharge experiment, another interesting feature of this device was observed. The piles of the cohesive materials formed at the discharge were very even, and the edges of the piles were very uniformed. This indicates that a small size MAPF unit could be used as an angle of repose measurement device. An example of the heaps formed by this device for powders such as cornstarch and lactose are shown in Fig. 8, indicating the ability of this device to produce very uniformed heaps of cohesive powders. Our extensive study [34] shows that this device can provide very reproducible results, the heaps formed do not have false peaks, the measurement of the angle of repose is very easy, and operator errors are minimized.

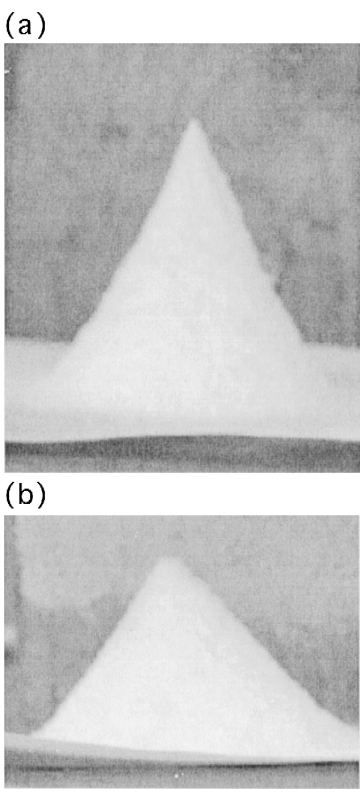

Fig. 8. Examples of heaps formed by discharge from MAPF device: (a) cornstarch, (b) lactose. Note that a clean, smooth pile has been obtained even for cornstarch, which has a high value of the angle of repose.

4. Simulation results

In this section, results from a preliminary simulation study are presented. The cases considered in this section were selected to provide a qualitative explanation of the experimental results presented in this paper and to examine the scalability of this approach. In this study, a rectangular simulation box of size $2.5 \times 2.5 \times 6$ cm was used. This size is selected to approximately match the experimental apparatus. Later in this section (see Section 4.3), we discuss the issue of the scale-up of this unit. Initially, the particles, magnetic and/or non-magnetic, were placed randomly throughout the box, and were allowed to fall under gravity. The inter-particle interactions, other than the magnetic ones, include a Hertz-like normal contact with a linear spring that has a different value of stiffness for loading and unloading [32], a Hertz-Mindlin type tangential compliance [33], and friction. The particles were considered to be non-cohesive.

We note that the magnetic field used in our simulations was assumed to be generated by an infinite solenoid. Thus, as may be observed from Eq. (6), if a single particle in the system was initially aligned with the direction of the magnetic flux, it would not experience any torque, and would remain at rest. The actual coils used in our experiments were not like a solenoid, and have a rotating magnetic field (direction of the field itself is rotating), thus the simulation results presented here represent a conservative case.

4.1. Simulation of the magnetic particles under various conditions

The first series of results consider the motion of the magnetic particles alone. While the behavior of the 1 g of magnets within 40 g of cornstarch would be much different than that of 1 g of magnets alone, these results show the nature of fluidization and the effect of various parameters on fluidization. First, we show the effect of varying the mass (or total amount) of magnets within the simulation box. The state of fluidization is shown by considering the number density distribution in the box. The box is divided into five horizontal cells, and the number density

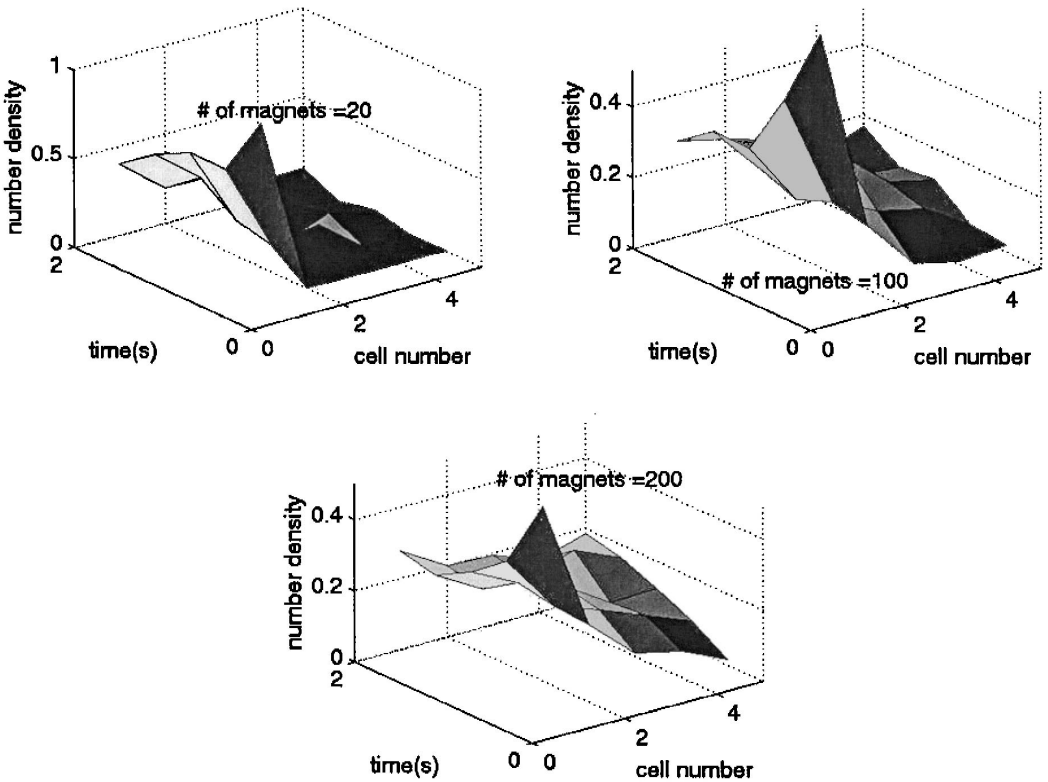

Fig. 9. Simulation results for number density evolution of the magnetic particles as a function of the total mass of magnets. Top left, 20 magnets; top right, 100 magnets; and bottom, 200 magnets. As the number of magnets is increased, the level of fluidization increases.

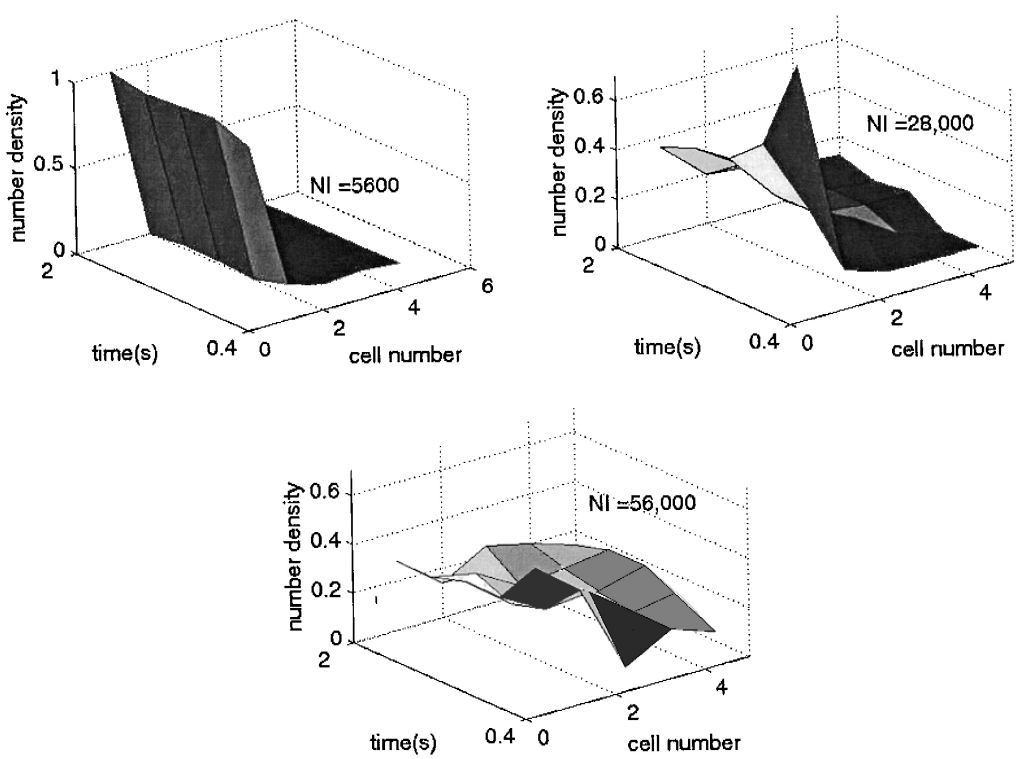

Fig. 10. Simulation results for number density evolution of the magnetic particles as a function of the magnetic field strength (varied by changing the number of turns in the coil). Top left, $NI = 5600$ A-turns/m; top right, $NI = 28\,000$ A-turns/m; and bottom, $NI = 56\,000$ A-turns/m. As the product NI is increased, the level of fluidization increases.

within each cell is computed as a function of time. Here, the number density values vary between 0 and 1, where the value of 1 for a given cell means that all the particles in the box are in that cell. Hence, a uniform distribution would be indicated by a constant value of 0.2 in each cell. In Fig. 9, three cases of the number of magnets within the box are considered, 20, 100, and 200 magnets (e.g., 100 magnets correspond to 3.2 g mass for a spherical particle of 2.36 mm). The time evolution of the number density is shown for each case. At each time, the results shown are instantaneous snap-shots of the number density distribution. As can be observed, the state of fluidization increases as the total mass of the magnet increases. Since the amount of fluidization may affect the flowability of the material to a great extent, these results are in line with the experimental results in Section 3.2 and in Fig. 5. Moreover, the time evolution indicates that the fluidization is fairly random and does not change significantly with time after 1 s. This in part may explain the ability of this device to obtain a constant flow rate as shown in Section 3.1 and in Fig. 4.

In Fig. 10, the effect of the magnetic flux density on fluidization is examined. The simulation cell was the same size and 50 magnets were placed in the cell. The flux density was varied by increasing the number of turns of the coil at a constant current of 5 A. Three cases are shown, 5600, 28 000, and 56 000 A-turns/m. Note that the scale of the plot in the last two cases is different from the first one. As can be expected, the state of fluidization, indicated by a more uniformed distribution of the magnets, is higher in the case of 56 000 A-turns/m. These results are in line with the results in Section 3.3 and in Fig. 6. It is noted that the state of fluidization denoted by the number density distribution is only one of several indications of increased flowability. Another way to increase the magnetic flux density is by increasing the current. This is shown in the next set of results, where instead of plotting the number density evolution, we plot the average number

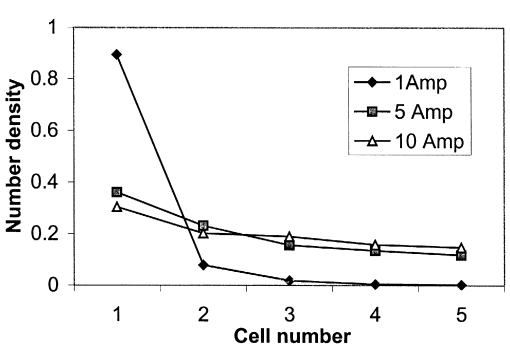

Fig. 11. Simulation results for the time-averaged number density of magnetic particles as a function of the magnetic field strength (varied by changing the current in the coil). The curve marked with diamonds is for 1 A, showing the least amount of fluidization, while the curves marked with squares and triangles are for 5 and 10 A, respectively, with much increased level of fluidization.

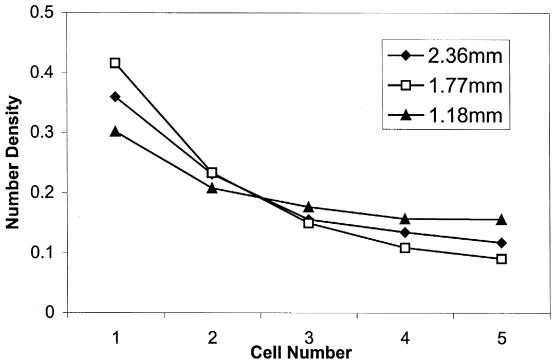

Fig. 12. Simulation results for the time-averaged number density of magnetic particles as a function of the size of the magnetic particles for a constant mass of magnets. The curve marked with triangles is for the smallest magnetic particle size (1.18 mm), showing the highest amount of fluidization, while the curves marked with squares and diamonds are for 1.77 and 2.36 mm A, respectively, with less fluidization.

density distributions during the simulation time period from 1 to 5 s. The results are plotted in Fig. 11, showing a distinct increase in fluidization as the current is increased. The increase in the fluidization from 5 to 10 A is less significant than as from 1 to 5 A. Next, the effect of varying the magnet size while keeping the total mass of the magnets constant is considered. Three magnet sizes were considered and the averaged number density distributions during the simulation time period from 1 to 5 s are plotted in Fig. 12. The total mass of the magnets in each case is the same, 1.6 g. These results indicate that one cannot determine the total effect of the change in magnetic particle size on the powder flow by looking at the fluidization of the magnets alone. More detailed investigation is required to fully corroborate with the experimental results shown in Fig. 7.

4.2. Simulation of the mixture of magnetic particles and non-magnetic particles

The second series of results are for the case of the mixture of magnetic and non-magnetic particles. This system has 50 magnetic particles and 1000 non-magnetic particles of density 1.19 g/cm^2 (magnets have a density of 4.7 g/cm^2). While the number ratio of magnetic and non-magnetic particles is not comparable to a real system such as was the case shown in Figs. 2 and 3, we can get some indication of the ability of magnets to fluidize non-magnets due to collisions. The results are shown in Fig. 13, where (a) shows the number density distribution of magnetic particles as a function of time (each of the three curves is at a different time), and (b) shows the same for the non-magnetic particles. Both types of particles are fluidized, however, at the end of the run (0.9 s), the magnets show very little fluidization, but they are able to fluidize the non-magnets. In these figures, it appears that

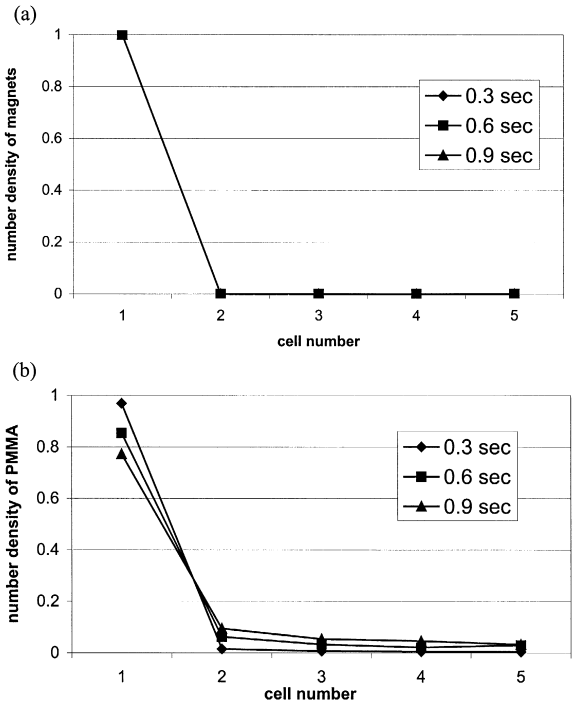

Fig. 13. Simulation results for number density evolution in a mixed system: (a) magnetic particles, (b) non-magnetic particles. As seen, the magnetic particles are all in the bottom zone, yet they are able to fluidize the non-magnetic particles.

when non-magnets are placed along with magnets, the fluidization level of the magnets significantly diminishes. However, for the flow of the non-magnets to occur, only a small level of agitation may be required. To understand how all the non-magnetic particles are affected, we present more results. In Fig. 14, the average of the displacement (normalized by the particle diameter) of 1000 non-magnets is plotted from time 0.2–0.3 s, indicating that within a time span of 0.1 s, the average displacement of non-magnets is as high as 6 to 8 particle diameters. Another plot, in Fig. 15, shows the cumulative number distribution of the amount of displacement experienced by 1000 non-magnets

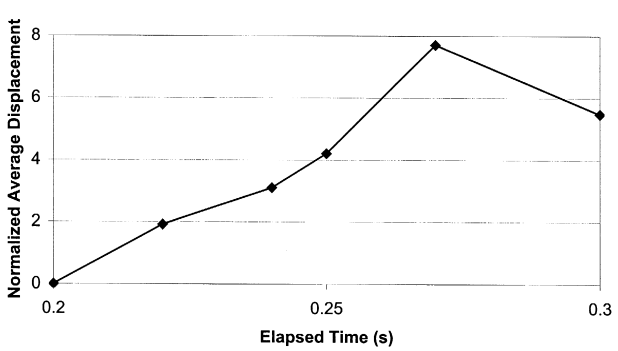

Fig. 14. Time evolution of normalized average displacement of 100 non-magnetic particles from simulation study of Fig. 13. The displacement is measured from each particle's position at time 0.2 s.

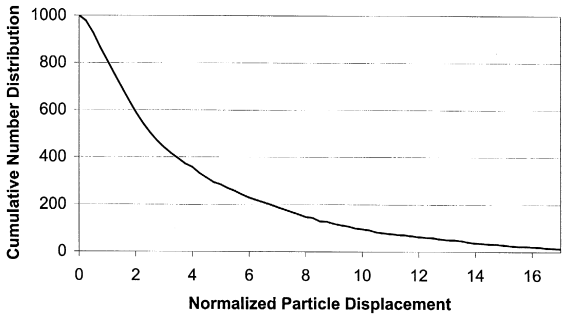

Fig. 15. Simulation results showing the number distribution of non-magnets undergoing the amount of displacement from time 0.2–0.25 s. The curve shows the number of particles that experiences the minimum amount of displacement, e.g., 600 particles have moved at least 2 particle diameters, while 100 particles have moved at least 10 particle diameters.

from time 0.2–0.25 s. As can be seen, the plot indicates that the majority of the particles, i.e., over 80%, moved more than 1 particle diameter during this time, while over half of them moved more than 2.5 particle diameters. Thus, these simulation results show that it is possible for the magnets to cause sufficient motion of the non-magnets so as to initiate powder flow. Please note that excessive computational time required in making these calculations has prevented us from running the simulation for a longer period of time. We anticipate that in a time period of about 1 s, most particles would have moved a much larger distance.

4.3. Simulation of the magnetic particles in scaled-up box sizes

As mentioned before, we have selected a simulation cell size that is comparable to the experimental apparatus. In this section, we show simulation results for larger cell/box sizes. In this device, when it is scaled up, there is no need to increase the size of the magnets to compensate for a larger apparatus size assuming that the powder material is the same. In other words, for the same powder material, there is no need for any direct relation between the particle size and the cell size. In fact, this is the advantage of this approach. However, in order to excite the larger mass of powder in a larger apparatus, one must have more magnetic particles as the powder volume goes up. It is then expected that in the scale up of this device, magnetic particle size, properties, and magnetic field will be kept the same, but the number of magnetic particles per unit volume will be kept constant, and accordingly the total number of magnetic particles will be increased as the box size goes up.

To illustrate this point, simulations were carried out for four different sizes of cells — the original size ($2.5 \times 2.5 \times 6$ cm), one and a half times each dimension (i.e., $3.75 \times 3.75 \times 9$ cm), doubling each dimension, and qua-

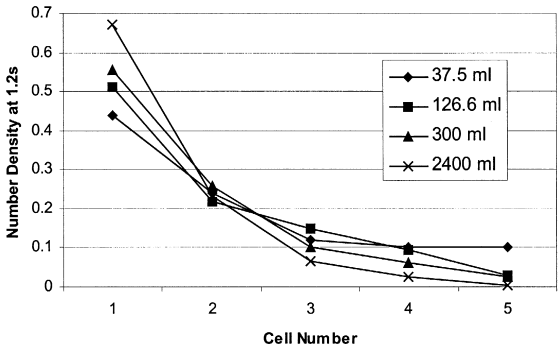

Fig. 16. Degree of fluidization after 1.2 s elapsed time in four different simulation cell sizes (size varies from 37.5 to 2400 ml). In each case, the number of magnets per unit volume is kept the same.

drupling each dimension. Thus, in terms of volume, they are the original volume and 3.375, 8 and 64 times the original volume, respectively. In each case, the total number of magnetic particles per unit volume is kept the same. To show that these systems are roughly equivalent in terms of magnetic excitation intensity, we have computed various diagnostic quantities; (1) the degree of fluidization, (2) average rotational velocity of the magnetic particles, and (3) average translational velocity of the magnetic particles for each cell size. The results for the degree of fluidization are shown in Fig. 16 after 1.2 s of elapsed time (the results at other times are similar). As can be seen, the differences between the results for different cell sizes are not significant, and the differences can be mostly attributed to wall-effects, because for smaller cells, the particles may travel a shorter distance before hitting a wall. Fig. 17 shows the time evolution of the rotational velocity averaged over all the magnets for each cell size. Here, the differences between the various cell sizes are insignificant. Fig. 18 shows the time evolution of translational velocity averaged over all the magnets for each cell size. In this case, the differences between various cell sizes are small and the larger cells show higher velocities. This behavior may also be attributed to wall-effects, as the particles in a larger cell may be able to travel further without hitting a wall. These three figures indicate that one can achieve essentially the

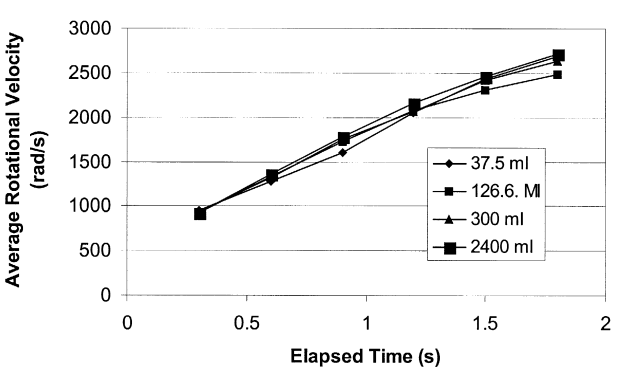

Fig. 17. Time evolution of rotational velocity averaged over all the magnets for each cell size of Fig. 16.

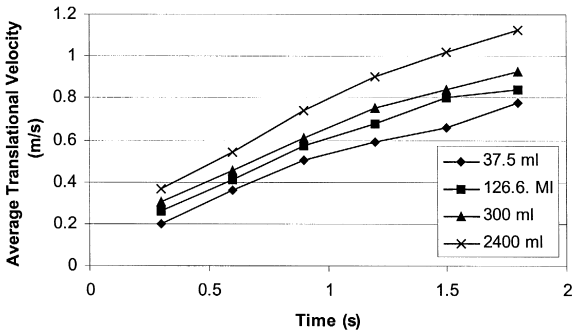

Fig. 18. Time evolution of translational velocity averaged over all the magnets for each cell size of Fig. 15.

same ''scale'' of magnetic fluidization and excitation by just keeping the number of particles per volume the same.

5. Discussion and conclusions

A novel powder fluidization technique is proposed based on the use of hard permanent magnets mixed with the powder and subjected to an oscillating magnetic field. This concept is used to develop the MAPF system, which is investigated for discharging cohesive powder from a hopper. The governing equations of motion and the numerical simulation results show that the magnets spin and move violently within the system, creating a state of fluidization. It is emphasized that Eq. (6) represents a highly non-linear dynamical system even for a few magnetic particles, but when a large number of particles are put together, a truly chaotic system is created. The animation of simulation results (not shown in the paper) indicates that a highly chaotic state is produced within the system. Furthermore, the simulation results show qualitative agreement with the experimental results.

Due the nature of the excitations created in this system, it is shown to be useful in stimulating powder discharge from hoppers. The effects of various operating parameters on the discharge rate are investigated, and it is shown that this device is capable of achieving constant discharge rates which may be controlled by either changing the amount of magnets used or by changing the magnetic field strength through change in input voltage. The size of the magnetic particles also affects the powder flow rate. An optimum size is observed to attain the maximum powder flow rate. The optimum value depends on the combination of the magnetic moment and the particle number concentration required to effectively overcome powder strength. The device may also be used as an angle of repose measurement system. Simulation results show a qualitative agreement with the experimental observations.

Next, we discuss the scale-up issues. We would like to point out, however, that we do not anticipate this device to be used for very large hoppers and silos. Nonetheless, it would be very useful for small batch (about 1000 to 2000

kg) high value-added applications. In principle, the scale-up for this device is relatively straightforward. That is so because one can potentially achieve the same level of powder excitation by ensuring that the magnetic field intensity is kept the same in a scaled-up device and the number of magnetic particles per unit volume is kept constant. This allows for the same level of powder excitation per unit volume. Simulation results in Section 4.3 show this to be true, as the magnetic excitation level in four different cell sizes is nearly the same when a constant amount of magnets per unit volume are used. In practice, however, one does not need to excite the whole volume of the hopper. Typically, one must excite the powder near the outlet of the hopper only. In that case, as the hopper size increases, the number of magnets should be increased only in proportion to the hopper outlet area and not the volume. Another issue is the magnetic field. The same magnitude of the magnetic field may be achieved in a larger coil by maintaining a constant value for the product of the number of turns per meter in the coil and the current in the coil, as per Eq. (2). Even for a finite solenoid, if the diameter to height ratio is kept the same, this relation is valid. Thus, this could be easily achieved in practice.

In terms of the power requirements for a scaled-up device, a simplified analysis is presented. The amount of power required consists of two parts. One part is the power needed to make the magnets move and the second part involves the losses in the field coil. In our experiments, no effort is made to optimize the field coil design, and in fact, a coil from a stator of A/C motor is used. Thus, it is expected to have large amount of losses. The power needed to make the magnets move is approximately proportional to the number of magnets, the magnetic moment of each particle, and the powder resistance that each magnet is trying to overcome. As shown in Section 4.3, the scale up of this device involves increasing the number of magnets so as to keep the number of magnets per unit volume constant. As the device gets larger, the powder resistance that a magnet has to overcome may increase slightly. Nevertheless, the main contribution to increase power requirement comes from the increase in the number of magnets, which is proportional to the volume of the scaled-up device. However, in a practical system, one may only increase the number of magnets in proportion to the hopper outlet size. Therefore, the power requirement does not become prohibitive in the sense that it scales about linearly with the hopper outlet. Regarding the losses in the field coil, they are proportional to the product of the supply voltage and the current in the coil. Equivalently, the power requirement is proportional to I^2R, where I is the current in the coil and R is the resistance of the coil. As mentioned before, to maintain the same magnetic field, one must keep the product of the current and number of turns per meter constant. Thus, the scale up does not necessarily require an increase in the current. However, as the size increases for the same value of NI (see Eq. (2)), the total length of the wire and hence its resistance increase in proportion to the product of the diameter, D, and height, H, of the coil. Thus, the power loss is proportional to DH and the power required to move the magnets is proportional to D^2. Therefore, as the device is scaled-up, the power requirement goes up approximately linearly with the hopper outlet area. Thus, the power requirements for the scaled-up device will not be prohibitive. In comparable techniques such as vibrations to enhance the flow, one must be able to provide sufficient energy to transmit the effect of wall or structure vibration to the powder bulk within the hopper. For example, in case of a bin activator, the power requirement would be proportional to the size of the inverted cone that is being vibrated. That size is directly proportional to the hopper outlet, and hence, the power requirement will also scale up linearly with the hopper outlet.

As mentioned before, most flow aids either reduce the wall friction or improve flowability of the cohesive powder (or do both). This device may reduce the wall friction near the exit through random collisions with the hopper wall and it increases material flowability by breaking the internal structure as well as by creating a fluidization effect on the cohesive powders. It is well known that if the powder is fluidized, it behaves very much like liquid [1]. This is the principal reason for the success of this device. In comparison to most commercial devices, MAPF most closely resembles the bin activators, which are designed to provide a ''live'' bottom to the hopper. However, the advantage of this device is that it has many point sources of agitation, hence, the mechanism of this device is different from bin activators and other existing devices, because in MAPF the agitations are created internally and throughout the exit zone of the hopper. Moreover, by modifications to the design of the magnetic field in MAPF, it may be possible to extend the magnetic excitations to penetrate well above the hopper outlet area. There are several advantages of this device as listed below.

- This device can produce uniform flow rates and is much less likely to flood due to the presence of a mesh.
- The nature of its fluidization suggests that this device would not promote compaction, which may be caused by vibrations.
- It does not require the internal support structure needed in most bin activators. As reported in Ref. [5], such support structures may hinder the powder flow.
- The chaotic agitations created by this device may promote fluidization, subsequent mixing, and should not cause segregation of the powder material.
- The noise level in this device would be significantly lower than vibratory devices or air blasters.

While there are several distinct advantages, a number of potential hurdles await successful utilization of this device.

First, in a scaled-up device, the size of the magnetic field coil and its effect on the surrounding area may become potential problems. Another problem is that ideally one should not use metallic materials in the operating areas of this device. While the magnetic field can pass through thin metallic (non-ferrous) objects, placement of heavy metallic, and in particular, ferromagnetic objects in the vicinity may give rise to a significant loss of the magnetic field and may require a very high level of applied magnetic field intensity. Thus, this device has several advantages as well as disadvantages and more development work is required for its scale-up.

In summary, a novel powder flow enhancement system is proposed, and through experimental results it is shown that it can achieve controlled discharge of cohesive powders in a small laboratory unit. Numerical simulation results reveal the nature of the fluidization in this device. While the results presented here are preliminary, they show that the device is attractive due to its unique flow enhancement mechanism, which is quite different from the existing techniques. The ability of MAPF to be used for flow enhancement of consolidated cohesive powders has been also investigated, see, for example, Ref. [35].

Acknowledgements

Financial support from the New Jersey Commission on Science and Technology through the Grant No. 97-100-020-2890-051-6130 is gratefully acknowledged. The authors also wish to thank Mr. Sanjiv Patel and Mr. Mariusz Maziarz, Chemical Engineering Department, NJIT, for performing the experiments; Mr. William Dunphy, Mechanical Engineering Department, NJIT, for setting up the experimental system; Mr. Greg James, Mechanical Engineering Department, NJIT, for providing the angle of repose results; and Dr. Maher Moakher and Dr. Fernando Muzzio for providing an object-oriented version of the original code from Ref. [33].

References

[1] A.W. Jenike, Storage and Flow of Solids, Bulletin No. 123 of the Utah Engineering Station, Salt Lake City, Utah, March 1970.
[2] Standard Shear Testing Technique for Particulate Solids Using the Jenike Shear Cell, A Report of the EFCE, The Institution of Chemical Engineers: Europian Federation of Chemical Engineering, Working Party on the Mechanics of Particulate Solids, 1989.
[3] G.D. Dumbaugh, The induced vertical flow of bulk solids from storage, Bulk Solids Handling 4 (1) (1984) 153–171.
[4] J.R. Johanson, Boosting and controlling fine powder flow rates, Powder Handling and Processing 5 (3) (1993) 273–276.
[5] J. Marinelli, J.W. Carson, Solve solids flow problems in bins, hoppers and feeders, Chemical Engineering Progress (1992) 22–28, May.
[6] H. Purutyan, B.H. Pittenger, J.W. Carson, Solve solids handling problems by retrofitting, Chemical Engineering Progress (1998) 27–39, April.
[7] A. Rappen, H. Wright, The use of air cannons to solve coal flow problems in both mass and core flow bunkers with specific reference to the phenomenon of silo quaking,Proceedings of 2nd International Conference on Design of Silos for Strength and Flow, Stratford-Upon-Avon, November 7–9, 1998, pp. 423–433.
[8] A.R. Reed, C.H. Duffell, A review of hopper discharge aids, Bulk Solids Handling 3 (1) (1983) 149–156.
[9] A.W. Roberts, Bulk solids handling: recent developments and future directions, Bulk Solids Handling 11 (1) (1991) 17–35.
[10] T.A. Royal, J.W. Carson, How to avoid flooding in powder handling systems, Bulk Solids Handling 5 (1) (1993) 63–67.
[11] P.A. Shamlou, Handling of Bulk Solids: Theory and Practice, Butterworth, London, 1988.
[12] D.H. Wilson, D.L. Dunnington, To avoid feeding problems, Chemical Engineering (1991) 73–81, August.
[13] C.R. Woodcock, J.S. Mason, Bulk Solids Handling, Chapman & Hall, New York, 1987.
[14] A.W. Roberts, M. Ooms, O.J. Scott, Influence of vibrations on the strength and boundary friction characteristics of bulk solids and the effect on bin design and performance, Bulk Solids Handling 6 (1) (1986) 161–169.
[15] E.R. Nowak, M. Povineli, H.M. Jaeger, S.R. Nagel, Studies of granular compaction, Powder and Grains 97 (1997) 377–380.
[16] C.R. Wassgren, C.E. Brennen, M.L. Hunt, Granular flow in a vertically vibrating hopper, Proceedings of the 10th Conference on Engineering Mechanics 2 (1995) 1111–1114.
[17] C.R. Wassgren, M.L. Hunt, C.E. Brennen, Effects of vertical vibration on hopper flows of granular material, in: C.S. Chang, A. Misra, R. Liang, M. Babic (Eds.), Mechanics of Deformation and Flow of Particulate Materials, ASCE, Reston, VA, 1997, pp. 335–348.
[18] H. Takahashi, A. Suzuki, T. Tanaka, Behavior of a particle bed in the field of vibration: I. Analysis of particle motion in a vibrating vessel, Powder Technology 2 (1968) 65–71.
[19] A. Suzuki, H. Takahashi, T. Tanaka, Behavior of a particle bed in the field of vibration: II. Flow of particles through slits in the bottom of a vibrating vessel, Powder Technology 2 (1968) 72–77.
[20] J.B. Knight, H.M. Jaeger, S.R. Nagel, Vibration-induced size separation in granular media: the convection connection, Physical Review Letters 70 (24) (1993) 3728–3731.
[21] R.C. Weathers, M.L. Hunt, C.E. Brennen, A.T. Lee, C.R. Wassgren, Effects of horizontal vibration on hopper flows of granular materials, in: C.S. Chang, A. Misra, R. Liang, M. Babic (Eds.), Mechanics of Deformation and Flow of Particulate Materials, ASCE, Reston, VA, 1997, pp. 349–360.
[22] G. Donsi, G. Ferrari, Powder Technology 65 (1991) 469.
[23] D.S. Dick, R.J. Hossfeld, Versatile BINSERT System Solves Wide range of Flow Problems,12th Annual Powder and Bulk Solids Conference, Rosemont, IL, May, 1987.
[24] R.E. Rosensweig, Science 204 (1979) 57.
[25] R.E. Rosensweig, Industrial & Engineering Chemistry Fundamentals 18 (3) (1979) 260.
[26] J.N. Kuznetsov, V.A. Abrosimov, US Patent 3,987,967, October 26, 1976.
[27] Y. Watanabe, M. Nakamura, US Patent 4,632,316, December 30, 1986.
[28] B. Halbedel, W. Mueller, R. Baudrich, D. Huelsenberg, US Patent 5,348,237, September 20, 1994.
[29] R.K. Singh, A. Ata, J. Fitz-Gerald, Y. Rabinovich, W. Hendrikson, Kona 15 (1997) 121.
[30] M. Ramlakhan, C.-Y. Wu, R. Dave, R. Pfeffer, Proceedings of the World Congress on Particle Technology 3, Brighton, UK,1998.
[31] O.R. Walton, R.L. Braun, Viscosity and temperature calculations for shearing assemblies of inelastic, frictional disks, Journal of Rheology 30 (1986) 949–980.

[32] O.R. Walton, Numerical simulation of inelastic, frictional particle–particle interactions, in: M.C. Roco (Ed.), Particulate Two-Phase Flow, Butterworth-Heinemann, Boston, 1992, pp. 884–911.
[33] O.R. Walton, Numerical simulation of inclined chute flows of monodisperse, inelastic, frictional spheres, Mechanics of Materials 16 (1993) 239–247.
[34] G. James, C.-Y. Wu, R.N. Davé, Measuring angle of repose using a magnetically assisted powder flow system, Advanced Technologies for Particle Processing: 1998 AlChE Conference Vol. 11998, pp. 488–494, November.
[35] C.Y. Wu, S. Watano, R.N. Dave, Powder Handling and Processing 10 (4) (1998) 357–361, October/December.